10th AIAA/ISSMO Multidisciplinary Analysis and Optimization Conference, 30 Aug - 1 Sep 2004, Albany, New York

Aero-Structural Wing Planform Optimization Using the Navier-Stokes Equations

Kasidit Leoviriyakit*, Sangho Kim†, and Antony Jameson‡
Stanford Univerisity, Stanford, CA, 94305-4035, USA

This paper describes the formulation of optimization techniques based on control theory for wing section and planform design in viscous compressible flow modeled by the Reynolds Averaged Navier-Stokes equations. Because the two disciplines that are relevant to this problem are aerodynamics and structures, an extension of a single to a multiple objective cost function is considered. A realistic model for the structural weight, which is sensitive to both planform variations and wing loading, is implemented. Results of optimizing a wing-fuselage of a commercial transport aircraft show a successful trade-off between the aerodynamic and structural cost functions, leading to meaningful wing planform designs. Results also indicate that large improvements in lift-to-drag ratio can be achieved without any penalty on the structural weight by stretching the span along with decreasing the sweep angle, thickening the wing-sections, and modifying the airfoil sections. Furthermore, by varying the weighting constants in the cost function, the "Pareto front" can be captured, broadening the design range of optimal shapes.

I. Introduction

TRADITIONALLY the process of wing design has been carried out by trial and error, relying on the intuition and experience of the designer. With currently available equipment and efficient numerical algorithm the turn-around for numerical simulations is becoming so rapid that it is feasible to use computational fluid dynamics (CFD) to examine an extremely large number of variations. However, it is not likely that repeated trials in an interactive design and analysis procedure can lead to a truly optimum design. In order to take full advantage of examining a very large design space the numerical simulations need to be combined with automatic search and optimization procedures. This can lead to automatic design methods which will fully realize the potential improvements in multidisciplinary optimization.

Gradient information can be computed using a variety of approaches such as the finite-difference method, the complex step method,[1] and automatic differentiation.[2] Unfortunately, their computational cost is still proportional to the number of design variables in the problem. An alternative is to treat the design problem as a control problem. This approach has dramatic computational cost advantages over the other methods. The foundations of control theory for systems governed by partial differential equations were laid by J.L. Lions.[3]

The control-theory approach is often called the adjoint method, since the necessary gradients are obtained via the solution of the adjoint equations of the governing equations. The adjoint method is extremely efficient since the computational expense incurred in the calculation of the complete gradient is effectively independent of the number of design variables. The only cost involved is the calculation of one flow solution and one adjoint solution whose complexity is similar to that of the flow solution. Control theory was applied to shape design for elliptic equations by Pironneau[4] and it was first used in transonic flow by Jameson.[5,6,7] Since then this method has become a popular choice for design problems involving fluid flow.[8,9,10,11] During

*Doctoral Candidate, Department of Aeronautics and Astronautics, AIAA Member
†Postdoctoral Fellow, Department of Aeronautics and Astronautics, AIAA Member
‡Thomas V. Jones Professor of Engineering, Department of Aeronautics and Astronautics, AIAA Member.

the last decade, the methods have been intensively developed and have been proved to be very effective for improving wing section shapes for fixed wing-planforms.[12,13]

In general the section shape changes needed for the transonic wing design are quite small. However, in order to obtain a true optimum design larger scale changes such as changes in the wing planform (sweepback, span, chord, section thickness, and taper) should be considered. Because these changes directly affect the structural weight, a meaningful result can only be obtained by considering a cost function that accounts for both the aerodynamic and structural characteristics.

Our previous works[14,15] validated a design methodology for wing section and planform optimization with simple estimation of wing weight, in both inviscid and viscous flow. We also extended our study[16] to validate a design methodology in inviscid flow with a more realistic structural-weight-model that was sensitive to changes of both geometry and aerodynamic load. In addition we also developed a large-scale adjoint method to calculate the planform gradients.

We found that if the cost function contained both aerodynamic and structural weight dependencies, the trade-off between these two dependencies would lead to a useful design. However, this raised the question of how to properly integrate these dependencies together. One practical way to solve the relative importance of aerodynamic and structural dependencies was to consider the overall performance, such as the maximum range of the aircraft.

We also found that while inviscid calculations were proven useful for the design of transonic wings at the cruise condition, the required changes in the section shape were comparable in magnitude to the displacement thickness of the boundary layer. Thus viscous design was more realistic, and alleviated shocks that would otherwise form in the viscous solution over the final inviscid design. Accurate resolution of viscous effects such as separation and shock/boundary layer interaction was also essential for optimal design encompassing off-design conditions.

In this work, we report improvements in a design for wing planform optimization based on compressible viscous flow calculation and a realistic structural weight model. We also consider an alternative approach to combine the aerodynamic and structural cost functions to cover a broader design range, based on the concept of the "Pareto front". Optimized results of a transonic long-range transport aircraft show that large improvements in lift-to-drag ratio can be achieved while meeting criteria of other disciplines by stretching span to reduce vortex drag, decreasing sweep and thickening wing section to reduce structural weight, and modifying airfoil sections to minimize the shock drag. This trend has been further investigated for general long-range transport aircraft and results are presented in reference.[17]

II. Mathematical formulation

A. Design using the Navier-Stokes equations

The application of control theory to aerodynamic design problems is illustrated in this section for the case of three-dimensional wing design using the compressible Navier-Stokes equations as the mathematical model. It proves convenient to denote the Cartesian coordinates and velocity components by x_1, x_2, x_3 and u_1, u_2, u_3, and to use the convention that summation over $i = 1$ to 3 is implied by a repeated index i. Then, the three-dimensional Navier-Stokes equations may be written as

$$\frac{\partial w}{\partial t} + \frac{\partial f_i}{\partial x_i} = \frac{\partial f_{vi}}{\partial x_i} \quad \text{in } \mathcal{D}, \tag{1}$$

where the state vector w, inviscid flux vector f and viscous flux vector f_v are described respectively by

$$w = \begin{Bmatrix} \rho \\ \rho u_1 \\ \rho u_2 \\ \rho u_3 \\ \rho E \end{Bmatrix}, \quad f_i = \begin{Bmatrix} \rho u_i \\ \rho u_i u_1 + p\delta_{i1} \\ \rho u_i u_2 + p\delta_{i2} \\ \rho u_i u_3 + p\delta_{i3} \\ \rho u_i H \end{Bmatrix},$$

$$f_{vi} = \left\{ \begin{array}{c} 0 \\ \sigma_{ij}\delta_{j1} \\ \sigma_{ij}\delta_{j2} \\ \sigma_{ij}\delta_{j3} \\ u_j\sigma_{ij} + k\frac{\partial T}{\partial x_i} \end{array} \right\}, \tag{2}$$

and δ_{ij} is the Kronecker delta function. Also,

$$p = (\gamma - 1)\,\rho \left\{ E - \frac{1}{2} u_i u_i \right\}, \tag{3}$$

and

$$\rho H = \rho E + p \tag{4}$$

where γ is the ratio of the specific heats. The viscous stresses may be written as

$$\sigma_{ij} = \mu \left(\frac{\partial u_i}{\partial x_j} + \frac{\partial u_j}{\partial x_i} \right) + \lambda \delta_{ij} \frac{\partial u_k}{\partial x_k}, \tag{5}$$

where μ and λ are the first and second coefficients of viscosity. The coefficient of thermal conductivity and the temperature are computed as

$$k = \frac{c_p \mu}{Pr}, \qquad T = \frac{p}{R\rho}, \tag{6}$$

where Pr is the Prandtl number, c_p is the specific heat at constant pressure, and R is the gas constant.

Using a transformation to a fixed computational domain, the Navier-Stokes equations can be written in the transformed coordinates as

$$\frac{\partial (Jw)}{\partial t} + \frac{\partial (F_i - F_{vi})}{\partial \xi_i} = 0 \quad \text{in } \mathcal{D}, \tag{7}$$

where the inviscid terms have the form

$$\frac{\partial F_i}{\partial \xi_i} = \frac{\partial}{\partial \xi_i} \left(S_{ij} f_j \right),$$

the viscous terms have the form

$$\frac{\partial F_{vi}}{\partial \xi_i} = \frac{\partial}{\partial \xi_i} \left(S_{ij} f_{vj} \right),$$

and $S_{ij} = JK_{ij}^{-1}$ represent the projection of the ξ_i cell face along the x_j axis.

The geometry changes are represented by changes δS_{ij} in the metric coefficients. Suppose we choose to minimize the cost function of a boundary integral

$$I = \int_{\mathcal{B}} \mathcal{M}(w, S)\, d\mathcal{B}_\xi + \int_{\mathcal{B}} \mathcal{N}(w, S)\, d\mathcal{B}_\xi$$

where $\mathcal{M}(w, S)$ could be an aerodynamic cost function, e.g. drag coefficient, and $\mathcal{N}(w, S)$ could be a structural cost function, e.g. structure weight. A shape change produces a variation in the flow solution δw and the metrics δS which in turn produce a variation in the cost function

$$\delta I = \int_{\mathcal{B}} \delta\mathcal{M}(w, S)\, d\mathcal{B}_\xi + \int_{\mathcal{B}} \delta\mathcal{N}(w, S)\, d\mathcal{B}_\xi,$$

with

$$\begin{aligned} \delta\mathcal{M} &= [\mathcal{M}_w]_I\, \delta w + \delta\mathcal{M}_{II}, \\ \delta\mathcal{N} &= [\mathcal{N}_w]_I\, \delta w + \delta\mathcal{N}_{II}, \end{aligned}$$

where we continue to use the subscripts I and II to distinguish between the contributions associated with the variation of the flow solution δw and those associated with the metric variations δS. Thus $[\mathcal{M}_w]_I$ and $[\mathcal{N}_w]_I$ represent $\frac{\partial \mathcal{M}}{\partial w}$ and $\frac{\partial \mathcal{N}}{\partial w}$ with the metrics fixed, while $\delta\mathcal{M}_{II}$ and $\delta\mathcal{N}_{II}$ represent the contribution of the metric variations δS to $\delta\mathcal{M}$ and $\delta\mathcal{N}$.

In the steady state, the constraint equation (7) specifies the variation of the state vector δw by

$$\frac{\partial}{\partial \xi_i}\delta\left(F_i - F_{vi}\right) = 0.$$

Here δF_i and δF_{vi} can also be split into contributions associated with δw and δS using the notation

$$\begin{aligned}\delta F_i &= \left[F_{i_w}\right]_I \delta w + \delta F_{i_{II}} \\ \delta F_{vi} &= \left[F_{vi_w}\right]_I \delta w + \delta F_{vi_{II}}.\end{aligned}$$

Multiplying by a costate vector ψ, which will play an analogous role to the Lagrange multiplier, and integrating over the domain produces

$$\int_{\mathcal{D}} \psi^T \frac{\partial}{\partial \xi_i}\delta\left(F_i - F_{vi}\right) d\mathcal{D}_\xi = 0.$$

If ψ is differentiable this may be integrated by parts to give

$$\int_{\mathcal{B}} n_i \psi^T \delta\left(F_i - F_{vi}\right) d\mathcal{B}_\xi - \int_{\mathcal{D}} \frac{\partial \psi^T}{\partial \xi_i}\delta\left(F_i - F_{vi}\right) d\mathcal{D}_\xi = 0. \tag{8}$$

Since the left hand expression equals zero, it may be subtracted from the variation in the cost function to give

$$\begin{aligned}\delta I &= \int_{\mathcal{B}} \left[\delta\mathcal{M} + \delta\mathcal{N} - n_i\psi^T\delta\left(F_i - F_{vi}\right)\right] d\mathcal{B}_\xi \\ &+ \int_{\mathcal{D}} \left[\frac{\partial \psi^T}{\partial \xi_i}\delta\left(F_i - F_{vi}\right)\right] d\mathcal{D}_\xi.\end{aligned} \tag{9}$$

Now, since ψ is an arbitrary differentiable function, it may be chosen in such a way that δI no longer depends explicitly on the variation of the state vector δw. The gradient of the cost function can then be evaluated directly from the metric variations without having to recompute the variation δw resulting from the perturbation of each design variable.

The variation δw may be eliminated from (9) by equating all field terms with subscript "I" to produce a differential adjoint system governing ψ

$$\frac{\partial \psi^T}{\partial \xi_i}\left[F_{i_w} - F_{vi_w}\right]_I = 0 \quad \text{in } \mathcal{D}. \tag{10}$$

The corresponding adjoint boundary condition is produced by equating the subscript "I" boundary terms in equation (9) to produce

$$n_i\psi^T\left[F_{i_w} - F_{vi_w}\right]_I = \left[\mathcal{M}_w\right]_I + \left[\mathcal{N}_w\right]_I \quad \text{on } \mathcal{B}. \tag{11}$$

The remaining terms from equation (9) then yield a simplified expression for the variation of the cost function which defines the gradient

$$\begin{aligned}\delta I &= \int_{\mathcal{B}} \left\{\delta\mathcal{M}_{II} + \delta\mathcal{N}_{II} - n_i\psi^T\left[\delta F_i - \delta F_{vi}\right]_{II}\right\} d\mathcal{B}_\xi \\ &+ \int_{\mathcal{D}} \left\{\frac{\partial \psi^T}{\partial \xi_i}\left[\delta F_i - \delta F_{vi}\right]_{II}\right\} d\mathcal{D}_\xi,\end{aligned} \tag{12}$$

Choosing ψ to satisfy the adjoint equation with appropriate boundary conditions depending on the cost function, the explicit dependence on δw is eliminated allowing the cost variations to be expressed in terms of δS and the adjoint solution, and hence finally in terms of the change $\delta\mathcal{S}$ in a function $\mathcal{S}(\xi)$ defining the shape.

Thus one obtains

$$\delta I = \int \mathcal{G}\delta\mathcal{S}\, d\xi = \langle \mathcal{G}, \delta\mathcal{S}\rangle$$

where $\mathcal{G}$ is the infinite dimensional gradient (Frechet derivative) at the cost of one flow and one adjoint solution. Then one can make an improvement by setting

$$\delta \mathcal{S} = -\lambda \mathcal{G}$$

In fact the gradient $\mathcal{G}$ is generally of a lower smoothness class than the shape $\mathcal{S}$. Hence it is important to restore the smoothness. This may be affected by passing to a Sobolev inner product of the form

$$\langle u, v \rangle = \int (uv + \epsilon \frac{\partial u}{\partial \xi} \frac{\partial v}{\partial \xi}) \, d\xi$$

This is equivalent to replacing $\mathcal{G}$ by $\bar{\mathcal{G}}$, where in one dimension

$$\bar{\mathcal{G}} - \frac{\partial}{\partial \xi} \epsilon \frac{\partial \bar{\mathcal{G}}}{\partial \xi} = \mathcal{G}, \quad \bar{\mathcal{G}} = \text{zero at end points}$$

and making a shape change $\delta \mathcal{S} = -\lambda \bar{\mathcal{G}}$.

B. Adjoint equations and boundary condition

Due to the additional level of derivatives in the stress and heat flux terms, it is proctical to derive the contributions form the inviscid and viscous terms separately.

In order to derive the adjoint equation in detail, equation (8) can be expanded as

$$\begin{aligned} &\int_{\mathcal{B}} \psi^T \left(\delta S_{2j} f_j + S_{2j} \delta f_j \right) d\mathcal{B}_\xi \\ &- \int_{\mathcal{D}} \frac{\partial \psi^T}{\partial \xi_i} \left(\delta S_{ij} f_j + S_{ij} \delta f_j \right) d\mathcal{D}_\xi \\ &- \int_{\mathcal{B}} \psi^T \left(\delta S_{2j} f_{vj} + S_{2j} \delta f_{vj} \right) d\mathcal{B}_\xi \\ &+ \int_{\mathcal{D}} \frac{\partial \psi^T}{\partial \xi_i} \left(\delta S_{ij} f_{vj} + S_{ij} \delta f_{vj} \right) d\mathcal{D}_\xi. \end{aligned} \tag{13}$$

It is convenient to assume that the shape modification is restricted to the coordinate surface $\xi_2 = 0$ so that $n_1 = n_3 = 0$, and $n_2 = 1$. Furthermore, it is assumed that the boundary contributions at the far field may either be neglected or else eliminated by a proper choice of boundary conditions as previously shown for the inviscid case.[18,19]

1. *Derivation of the Inviscid Adjoint Terms*

In equation (13) the inviscid flux variation can be expanded by setting

$$S_{ij} \delta f_j = S_{ij} \frac{\partial f_j}{\partial w} \delta w.$$

Taking the transpose of equation (13), it can be seen that in order to eliminate the explicit dependence on δw in the absence of viscous effect, ψ should be chosen to satisfy the inviscid adjoint equation

$$C_i^T \frac{\partial \psi}{\partial \xi_i} = 0 \quad \text{in } \mathcal{D}, \tag{14}$$

where the inviscid Jacobian matrices in the transformed space are given by

$$C_i = S_{ij} \frac{\partial f_j}{\partial w}.$$

In order to design a shape which will lead to a desired pressure distribution, natural choice is to set

$$I = \frac{1}{2} \int_{\mathcal{B}} (p - p_d)^2 \, dS$$

where p_d is the desired surface pressure, and the integral is evaluated over the actual surface area. In the computational domain this is transformed to

$$I = \frac{1}{2}\iint_{\mathcal{B}_w} (p - p_d)^2 \, |S_2| \, d\xi_1 d\xi_3,$$

where the quantity

$$|S_2| = \sqrt{S_{2j} S_{2j}}$$

denotes the face area corresponding to a unit element of face area in the computational domain. Now, to cancel the dependence of the boundary integral on δp, the adjoint boundary condition reduces to

$$\psi_j n_j = p - p_d \tag{15}$$

where n_j are the components of the surface normal

$$n_j = \frac{S_{2j}}{|S_2|}.$$

This amounts to a transpiration boundary condition on the co-state variables corresponding to the momentum components. Note that it imposes no restriction on the tangential component of ψ at the boundary.

2. Derivation of the Viscous Adjoint Equations

The viscous terms are derived below under the assumption that the viscosity and heat conduction coefficients μ and k are essentially independent of the flow, and that their variations may be neglected. This simplification has been successfully used for may aerodynamic problems of interest. However, if the flow variations could result in significant changes in the turbulent viscosity, it may be necessary to account for its variation in the calculation.

The derivation of the viscous adjoint terms can be simplified by transforming to the primitive variables

$$\tilde{w}^T = (\rho, u_1, u_2, u_3, p),$$

because the viscous stresses depend on the velocity derivatives $\frac{\partial u_i}{\partial x_j}$, while the heat flux can be expressed as

$$\kappa \frac{\partial}{\partial x_i}\left(\frac{p}{\rho}\right).$$

where $\kappa = \frac{k}{R} = \frac{\gamma\mu}{Pr(\gamma-1)}$. The relationship between the conservative and primitive variations is defined by the expressions

$$\delta w = M \delta \tilde{w}, \quad \delta \tilde{w} = M^{-1} \delta w$$

which make use of the transformation matrices $M = \frac{\partial w}{\partial \tilde{w}}$ and $M^{-1} = \frac{\partial \tilde{w}}{\partial w}$. These matrices are provided in transposed form for future convenience

$$M^T = \begin{bmatrix} 1 & u_1 & u_2 & u_3 & \frac{u_i u_i}{2} \\ 0 & \rho & 0 & 0 & \rho u_1 \\ 0 & 0 & \rho & 0 & \rho u_2 \\ 0 & 0 & 0 & \rho & \rho u_3 \\ 0 & 0 & 0 & 0 & \frac{1}{\gamma-1} \end{bmatrix}$$

$$M^{-1^T} = \begin{bmatrix} 1 & -\frac{u_1}{\rho} & -\frac{u_2}{\rho} & -\frac{u_3}{\rho} & \frac{(\gamma-1)u_i u_i}{2} \\ 0 & \frac{1}{\rho} & 0 & 0 & -(\gamma-1)u_1 \\ 0 & 0 & \frac{1}{\rho} & 0 & -(\gamma-1)u_2 \\ 0 & 0 & 0 & \frac{1}{\rho} & -(\gamma-1)u_3 \\ 0 & 0 & 0 & 0 & \gamma-1 \end{bmatrix}.$$

The conservative and primitive adjoint operators L and $\tilde{L}$ corresponding to the variations δw and $\delta\tilde{w}$ are then related by

$$\int_{\mathcal{D}} \delta w^T L\psi \; d\mathcal{D}_\xi = \int_{\mathcal{D}} \delta\tilde{w}^T \tilde{L}\psi \; d\mathcal{D}_\xi,$$

with

$$\tilde{L} = M^T L,$$

so that after determining the primitive adjoint operator by direct evaluation of the viscous portion of equation (13), the conservative operator may be obtained by the transformation $L = {M^{-1}}^T \tilde{L}$. Since the continuity equation contains no viscous terms, it makes no contribution to the viscous adjoint system. Therefore, the derivation proceeds by first examining the adjoint operators arising from the momentum equations and then the energy equation. The details may be found in.[20]

In order to make use of the summation convention, it is convenient to set $\psi_{j+1} = \phi_j$ for $j = 1, 2, 3$ and $\psi_5 = \theta$. Collecting together the contributions from the momentum and energy equations, the viscous adjoint operator in primitive variables can be finally expressed as

$$\begin{aligned}
(\tilde{L}\psi)_1 &= -\tfrac{p}{\rho^2}\tfrac{\partial}{\partial\xi_l}\left(S_{lj}\kappa\tfrac{\partial\theta}{\partial x_j}\right) \\
(\tilde{L}\psi)_{i+1} &= \tfrac{\partial}{\partial\xi_l}\left\{S_{lj}\left[\mu\left(\tfrac{\partial\phi_i}{\partial x_j}+\tfrac{\partial\phi_j}{\partial x_i}\right)+\lambda\delta_{ij}\tfrac{\partial\phi_k}{\partial x_k}\right]\right\} \\
&+ \tfrac{\partial}{\partial\xi_l}\left\{S_{lj}\left[\mu\left(u_i\tfrac{\partial\theta}{\partial x_j}+u_j\tfrac{\partial\theta}{\partial x_i}\right)\lambda\delta_{ij}u_k\tfrac{\partial\theta}{\partial x_k}\right]\right\} \\
&- \sigma_{ij}S_{lj}\tfrac{\partial\theta}{\partial\xi_l} \qquad\qquad \text{for} \quad i = 1, 2, 3 \\
(\tilde{L}\psi)_5 &= \tfrac{1}{\rho}\tfrac{\partial}{\partial\xi_l}\left(S_{lj}\kappa\tfrac{\partial\theta}{\partial x_j}\right).
\end{aligned}$$

The conservative viscous adjoint operator may now be obtained by the transformation

$$L = {M^{-1}}^T \tilde{L}.$$

Finally, the resulting adjoint equations for the Navier-Stokes equations are as follows:

$$C_i^T \frac{\partial\psi}{\partial\xi_i} - {M^{-1}}^T \tilde{L}\psi = 0 \quad \text{in } \mathcal{D}. \tag{16}$$

The first and the second terms come from the convective and diffusive terms of the Navier-Stokes equations respectively. The adjoint equation, a linear set of equations, is solved by marching the costate variables in time after a time-like derivative has been added.

3. *Viscous Adjoint Boundary Conditions*

The boundary term that arises from the momentum equations including both the δw and δS components equation (13) takes the form

$$\int_{\mathcal{B}} \phi_k \delta\left(S_{2j}\left(\delta_{kj}p + \sigma_{kj}\right)\right) d\mathcal{B}_\xi.$$

Replacing the metric term with the corresponding local face area S_2 and unit normal n_j defined by

$$|S_2| = \sqrt{S_{2j}S_{2j}}, \quad n_j = \frac{S_{2j}}{|S_2|}$$

then leads to

$$\int_{\mathcal{B}} \phi_k \delta\left(|S_2|\, n_j\left(\delta_{kj}p + \sigma_{kj}\right)\right) d\mathcal{B}_\xi.$$

Defining the components of the total surface stress as

$$\tau_k = n_j\left(\delta_{kj}p + \sigma_{kj}\right)$$

and the physical surface element

$$dS = |S_2|\, d\mathcal{B}_\xi,$$

the integral may then be split into two components

$$\int_{\mathcal{B}} \phi_k \tau_k \left|\delta S_2\right| d\mathcal{B}_\xi + \int_{\mathcal{B}} \phi_k \delta\tau_k dS, \tag{17}$$

where only the second term contains variations in the flow variables and must consequently cancel the δw terms arising in the cost function. The first term will appear in the expression for the gradient.

A general expression for the cost function that allows cancellation with terms containing $\delta\tau_k$ has the form

$$I = \int_{\mathcal{B}} \mathcal{I}(\tau) dS, \tag{18}$$

corresponding to a variation

$$\delta I = \int_{\mathcal{B}} \frac{\partial \mathcal{I}}{\partial \tau_k} \delta\tau_k dS,$$

for which cancellation is achieved by the adjoint boundary condition

$$\phi_k = \frac{\partial \mathcal{I}}{\partial \tau_k}.$$

Natural choices for $\mathcal{I}$ arise from force optimization and as measures of the deviation of the surface stresses from desired target values.

The force in a direction with cosines q_i has the form

$$C_q = \int_{\mathcal{B}} q_i \tau_i dS.$$

If we take this as the cost function (18), this quantity gives

$$\mathcal{I} = q_i \tau_i.$$

Cancellation with the flow variation terms in equation (17) therefore mandates the adjoint boundary condition

$$\phi_k = q_k.$$

Note that this choice of boundary condition also eliminates the first term in equation (17) so that it need not be included in the gradient calculation.

In the inverse design case, where the cost function is intended to measure the deviation of the surface stresses from some desired target values, a suitable definition is

$$\mathcal{I}(\tau) = \frac{1}{2} a_{lk} \left(\tau_l - \tau_{dl}\right) \left(\tau_k - \tau_{dk}\right),$$

where τ_d is the desired surface stress, including the contribution of the pressure, and the coefficients a_{lk} define a weighting matrix. For cancellation

$$\phi_k \delta\tau_k = a_{lk} \left(\tau_l - \tau_{dl}\right) \delta\tau_k.$$

This is satisfied by the boundary condition

$$\phi_k = a_{lk} \left(\tau_l - \tau_{dl}\right). \tag{19}$$

Assuming arbitrary variations in $\delta\tau_k$, this condition is also necessary.

In order to control the surface pressure and normal stress one can measure the difference

$$n_j \left\{\sigma_{kj} + \delta_{kj} \left(p - p_d\right)\right\},$$

where p_d is the desired pressure. The normal component is then

$$\tau_n = n_k n_j \sigma_{kj} + p - p_d,$$

so that the measure becomes

$$\begin{aligned}\mathcal{I}(\tau) &= \frac{1}{2}\tau_n^2 \\ &= \frac{1}{2}n_l n_m n_k n_j \left\{\sigma_{lm} + \delta_{lm}\left(p - p_d\right)\right\} \\ &\quad * \left\{\sigma_{kj} + \delta_{kj}\left(p - p_d\right)\right\}.\end{aligned}$$

This corresponds to setting

$$a_{lk} = n_l n_k$$

in equation (19). Defining the viscous normal stress as

$$\tau_{vn} = n_k n_j \sigma_{kj},$$

the measure can be expanded as

$$\begin{aligned}\mathcal{I}(\tau) &= \frac{1}{2}n_l n_m n_k n_j \sigma_{lm}\sigma_{kj} \\ &\quad + \frac{1}{2}\left(n_k n_j \sigma_{kj} + n_l n_m \sigma_{lm}\right)\left(p - p_d\right) \\ &\quad + \frac{1}{2}\left(p - p_d\right)^2 \\ &= \frac{1}{2}\tau_{vn}^2 + \tau_{vn}\left(p - p_d\right) + \frac{1}{2}\left(p - p_d\right)^2.\end{aligned}$$

For cancellation of the boundary terms

$$\begin{aligned}\phi_k\left(n_j \delta\sigma_{kj} + n_k \delta p\right) &= \left\{n_l n_m \sigma_{lm} + n_l^2\left(p - p_d\right)\right\} n_k \\ &\quad * \left(n_j \delta\sigma_{kj} + n_k \delta p\right)\end{aligned}$$

leading to the boundary condition

$$\phi_k = n_k\left(\tau_{vn} + p - p_d\right).$$

In the case of high Reynolds number, this is well approximated by the equations

$$\phi_k = n_k\left(p - p_d\right), \tag{20}$$

which should be compared with the single scalar equation derived for the inviscid boundary condition (15). In the case of an inviscid flow, choosing

$$\mathcal{I}(\tau) = \frac{1}{2}\left(p - p_d\right)^2$$

requires

$$\phi_k n_k \delta p = \left(p - p_d\right) n_k^2 \delta p = \left(p - p_d\right)\delta p$$

which is satisfied by equation (20), but which represents an over-specification of the boundary condition since only the single condition (15) needs be specified to ensure cancellation.

The form of the boundary terms arising from the energy equation depends on the choice of temperature boundary condition at the wall. For the adiabatic case, the boundary contribution is

$$\int_{\mathcal{B}} k\delta T \frac{\partial\theta}{\partial n} d\mathcal{B}_\xi,$$

while for the constant temperature case the boundary term is

$$\int_{\mathcal{B}} k\theta \left\{\frac{{S_{2_j}}^2}{J}\frac{\partial}{\partial\xi_2}\delta T + \delta\left(\frac{{S_{2_j}}^2}{J}\right)\frac{\partial T}{\partial\xi_2}\right\} d\mathcal{B}_\xi\ .$$

one possibility is to introduce a contribution into the cost function which depends on T or $\frac{\partial T}{\partial n}$ so that the appropriate cancellation would occur. Since there is little physical intuition to guide the choice of such a cost function for aerodynamic design, a more natural solution is to set

$$\theta = 0$$

in the constant temperature case or

$$\frac{\partial \theta}{\partial n} = 0$$

in the adiabatic case. Note that in the constant temperature case, this choice of θ on the boundary would also eliminate the boundary metric variation terms in

$$\int_{\mathcal{B}} \theta \delta \left(S_{2j} Q_j \right) d\mathcal{B}_\xi.$$

III. Implementation

A. Planform design variables

In this work, we model the wing of interest using six planform variables: root chord (c_1), mid-span chord (c_2), tip chord (c_3), span (b), sweepback(Λ), and wing thickness ratio (t), as shown in figure 1. This choice of

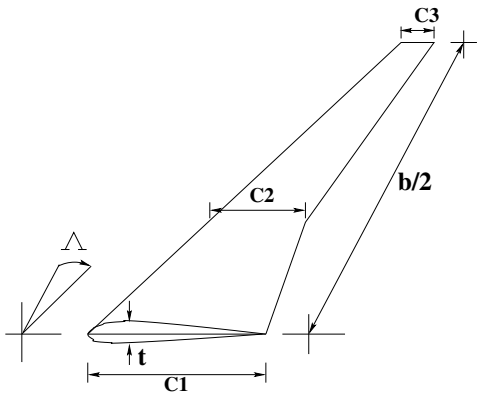

Figure 1. Modeled wing governed by six planform variables; root chord (c_1), mid-span chord (c_2), tip chord (c_3), span (b), and sweepback(Λ), wing thickness ratio (t).

design parameters will lead to an optimum wing shape that will not require an extensive structural analysis and can be manufactured effectively.

B. Cost function for planform design

In order to design a high performance transonic wing, which will lead to a desired pressure distribution, and still maintain a realistic shape, the natural choice is to set

$$I = \alpha_1 C_D + \alpha_2 \frac{1}{2} \int_{\mathcal{B}} (p - p_d)^2 dS + \alpha_3 C_W \tag{21}$$

where $C_W \equiv \frac{W}{q_\infty S_{ref}}$ is a dimensionless measure of the wing weight, which can be estimated either from statistical formulas, or from a simple analysis of a representative structure, allowing for failure modes such as panel buckling. The coefficient α_2 is introduced to provide the designer some control over the pressure distribution, while the relative importance of drag and weight are represented by the coefficients α_1 and α_3. The choice of these weighting constants is discussed in detainl in section F.

C. Structural weight model

To estimate $\mathcal{W}_{wing}$, a realistic model should account for both planform geometry and wing loading, but it should be simplified enough that we can express it as an analytical function.

An analytical model to estimate the minimal material to resist material and buckling failures has been developed by Wakayama.[21] When shear and buckling effects are small, they may be neglected, resulting in a simplified model developed by Kroo.[22] In this paper, we follow the analysis developed by Kroo.

The wing structure is modeled by a structure box, whose major structural material is the box skin. The skin thickness (t_s) varies along the span and resists the bending moment caused by the wing lift. Then, the structural wing weight can be calculated based on material of the skin.

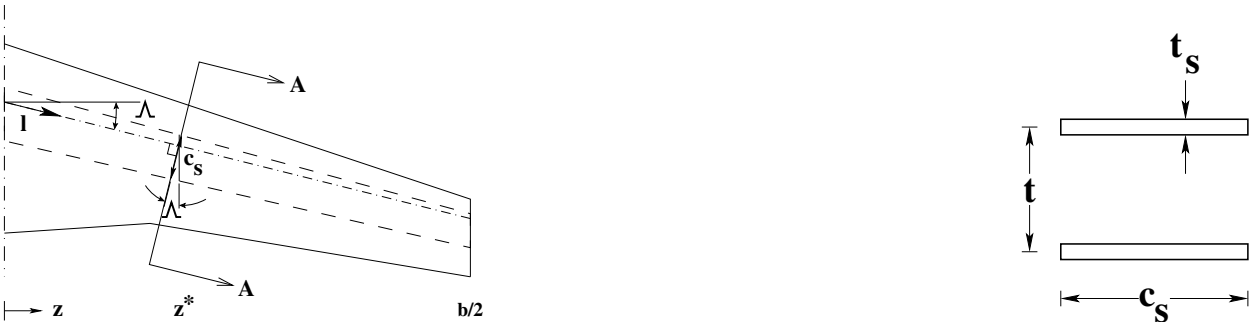

(a) swept wing planform

(b) section A-A

Figure 2. Structural model for a swept wing

Consider a box structure of a swept wing whose quarter-chord swept is Λ and its cross-section A-A as shown in figures 2. The skin thickness t_s, structure box chord c_s, and overall thickness t vary along the span. The maximum normal stress from the bending moment at a section z^* is

$$\sigma = \frac{M(z^*)}{tt_s c_s}$$

The corresponding wing structural weight is

$$\begin{aligned} \mathcal{W}_{wing} &\propto \int_{structual\ span} \frac{M}{t} dl \\ &= 2\frac{\rho_{mat} g}{\sigma cos(\Lambda)} \int_{-\frac{b}{2}}^{\frac{b}{2}} \frac{M(z^*)}{t(z^*)} dz^* \\ &= 4\frac{\rho_{mat} g}{\sigma cos(\Lambda)} \int_{0}^{\frac{b}{2}} \frac{M(z^*)}{t(z^*)} dz^*, \end{aligned}$$

and

$$C_W = \frac{\beta}{cos(\Lambda)} \int_0^{\frac{b}{2}} \frac{M(z^*)}{t(z^*)} dz^*, \tag{22}$$

where

$$\beta = \frac{4\rho_{mat} g}{\sigma q_\infty S_{ref}},$$

ρ_{mat} is the material density, and g is the gravitational constant.

The bending moment can be calculated by integrating pressure toward the wing tip.

$$\begin{aligned} M(z^*) &= -\int_{z^*}^{\frac{b}{2}} \frac{p(x,z)(z-z^*)}{cos(\Lambda)} dA \\ &= -\int_{z^*}^{\frac{b}{2}} \oint_{wing} \frac{p(x,z)(z-z^*)}{cos(\Lambda)} dx dz \end{aligned}$$

Thus

$$C_W = \frac{-\beta}{cos(\Lambda)^2} \int_0^{\frac{b}{2}} \int_{z^*}^{\frac{b}{2}} \oint_{wing} \frac{p(x,z)(z-z^*)}{t(z^*)} dx dz dz^* \tag{23}$$

To form the corresponding adjoint boundary condition, C_W must be expressed as $\int_{\mathcal{B}} d\mathcal{B}_\xi$ in the computational domain, or $\int\int dxdz$ in a physical domain to match the boundary term arise from the flow equations.

To switch the order of integral of (23), introduce a Heaviside function

$$H(z-z^*) = \begin{cases} 0, & z < z^* \\ 1, & z > z^* \end{cases}$$

Then (23) can be rewritten as

$$\begin{aligned} C_W &= \frac{-\beta}{cos(\Lambda)^2} \cdot \\ &\quad \int_0^{\frac{b}{2}} \int_0^{\frac{b}{2}} \oint_{wing} \frac{p(x,z)H(z-z^*)(z-z^*)}{t(z^*)} dxdzdz^* \\ &= \frac{-\beta}{cos(\Lambda)^2} \int_0^{\frac{b}{2}} \oint_{wing} p(x,z)K(z)dxdz, \end{aligned} \tag{24}$$

where

$$\begin{aligned} K(z) &= \int_0^{\frac{b}{2}} \frac{H(z-z^*)(z-z^*)}{t(z^*)} dz^* \\ &= \int_0^z \frac{z-z^*}{t(z^*)} dz^* \end{aligned}$$

In the computational domain,

$$C_W = \frac{-\beta}{cos(\Lambda)^2} \oint_{\mathcal{B}} p(\xi_1, \xi_3)K(\xi_3)S_{22}d\xi_1 d\xi_3, \tag{25}$$

and $K(\xi_3)$ is a one-to-one mapping of $K(z)$.

D. Adjoint boundary condition for the structural weight

For simplicity, it is assumed that the portion of the boundary that undergoes shape modifications is restricted to the coordinate $\xi_2 = 0$. Then equation (13) may be simplified by incorporating the conditions

$$n_1 = n_3 = 0, \quad n_2 = 1 \quad and \quad d\mathcal{B}_\xi = d\xi_1 d\xi_3,$$

so that the only variation δF_2 needs to be considered at the wall boundary. Moreover, the condition that there is no flow through the wall boundary at $\xi_2 = 0$ is equivalent to

$$U_2 = 0,$$

and

$$\delta U_2 = 0$$

when the boundary shape is modified. Consequently,

$$\delta F_2 = \delta p \begin{Bmatrix} 0 \\ S_{21} \\ S_{22} \\ S_{23} \\ 0 \end{Bmatrix} + p \begin{Bmatrix} 0 \\ \delta S_{21} \\ \delta S_{22} \\ \delta S_{23} \\ 0 \end{Bmatrix}. \tag{26}$$

The variation of C_W is

$$\delta C_W = -\beta \oint_{\mathcal{B}} \delta p \frac{KS_{22}}{cos(\Lambda)^2} + p\delta \left(\frac{KS_{22}}{cos(\Lambda)^2} \right) d\xi_1 d\xi_3, \tag{27}$$

Since δF_2 and δC_W depend only on the pressure, it allows a complete cancellation of dependency of the boundary integral on δp, and the adjoint boundary condition reduces to

$$\psi_2 S_{21} + \psi_3 S_{22} + \psi_4 S_{23} = \frac{-\beta}{cos(\Lambda)^2} KS_{22} \tag{28}$$

E. Gradient calculation for planform variables

The gradient with respect to planform variation can be computed by integrating point-gradients projected in the planform movement direction. If one chooses ψ as ψ^*, where ψ^* satisfies the adjoint equation (16) then

$$\begin{aligned}
\delta I(w,S) &= \delta I(S) \\
&= \int_{\mathcal{B}} \left(\delta\mathcal{M}_{II} + \delta\mathcal{N}_{II}\right) d\mathcal{B}_\xi + \int_{\mathcal{D}} {\psi^*}^T \delta R \, d\mathcal{D}_\xi \\
&\approx \sum_{\mathcal{B}} \left(\delta\mathcal{M}_{II} + \delta\mathcal{N}_{II}\right) \Delta\mathcal{B} + \sum_{\mathcal{D}} {\psi^*}^T \Delta\bar{R} \\
&\approx \sum_{\mathcal{B}} \left(\delta\mathcal{M}_{II} + \delta\mathcal{N}_{II}\right) \Delta\mathcal{B} \\
&+ \sum_{\mathcal{D}} {\psi^*}^T \left(\bar{R}|_{S+\delta S} - \bar{R}|_S\right),
\end{aligned}$$

where $\bar{R}|_S$ and $\bar{R}|_{S+\delta S}$ are volume weighted residuals calculated at the original mesh and at the mesh perturbed in the design direction.

Provided that ψ^* has already been calculated and $\bar{R}$ can be easily calculated, the gradient of the planform variables can be computed effectively by first perturbing all the mesh points along the direction of interest. For example, to calculate the gradient with respect to the sweepback, move all the points on the wing surface as if the wing were pushed backward and also move all other associated points in the computational domain to match the new location of points on the wing. Then re-calculate the residual value and subtract the previous residual value from the new value to form $\Delta\bar{R}$. Finally, to calculate the planform gradient, multiply $\Delta\bar{R}$ by the costate vector and add the contribution from the boundary terms.

This way of calculating the planform gradient exploits the full benefit of knowing the value of adjoint variables ψ^* with no extra cost of flow or adjoint calculations.

F. Choice of weighting constants

1. *Maximizing range of the aircraft*

The choice of α_1 and α_3 greatly affects the optimum shape. If $\frac{\alpha_3}{\alpha_1}$ is high enough, the optimum shape will have lower C_D and higher C_W than another optimum shape with lower $\frac{\alpha_3}{\alpha_1}$ value.

Leoviriyakit and Jameson[14] propose an intuitive choice of α_1 and α_3 by equating a problem of maximizing range of an aircraft to a problem of minimizing the cost function

$$I = C_D + \frac{\alpha_3}{\alpha_1} C_W.$$

If the simplified Breguet range equation can be expressed as

$$R = \frac{V}{C}\frac{L}{D} log \frac{W_1}{W_2}$$

where C is specific fuel consumption, D is drag, L is lift, R is range, V is aircraft velocity, W_1 is take off weight, and W_2 is landing weight, then choosing

$$\frac{\alpha_3}{\alpha_1} = \frac{C_D}{C_{W_2} log \frac{C_{W_1}}{C_{W_2}}}, \tag{29}$$

corresponds to maximizing the range of the aircraft.

2. *Pareto Front*

In order to present the designer with a wider range of choices, the problem of optimizing both drag and weight can be treated as a multi-objective optimization problem. In this sense one may also view the problem as a "game", where one player tries to minimize C_D and the other tries to minimize C_W. In order to compare the performance of various trial designs, designated by the symbol X in figure 3, they may be ranked for both drag and weight. A design is undominated if it is impossible either to reduce the drag for the same weight or to reduce the weight for the same drag. Any dominated point should be eliminated, leaving a set of undominated points which form the Pareto front. In figure 3, for example, the point Q is dominated by the point P (same drag, less weight) and also the point R (same weight, less drag). So the point Q will be eliminated. The Pareto front can be fit through the points P, R and other dominating points, which may be generated by using an array of different values of α_1 and α_3 in the cost function to compute different optimum shapes. With the aid of the Pareto front the designer will have freedom to pick the most useful design.

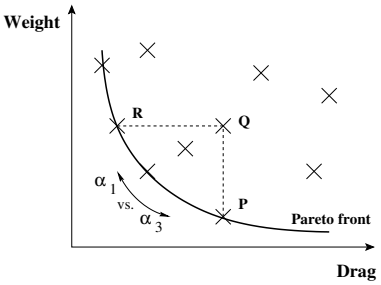

Figure 3. Cooperative game strategy with drag and weight as players

IV. Design cycle and parallel computation

In general, the computational cost of viscous design is at least one order of magnitude greater that the cost of inviscid design. Three main reasons for this are the increase of the number of grid points by a factor of two or more to resolve the boundary layer, the additional cost of computing the viscous terms and turbulent model, and a slower convergence due to highly stretched cells inside the boundary layers.

To make the design method feasible in practice, parallel computing is implemented to parts of the design cycle that dominate the computation time. Both flow and adjoint calculation have been implemented in a parallel setting using the message passing interface (MPI).

The design cycle starts by first solving the flow field until at least a 3 order of magnitude drop in the residual is achieved. The flow solution is then passed to the adjoint solver. Second, the adjoint solver is run to calculate the costate vector. Iteration continues until at least a 2 order of magnitude drop in the residual.[a] The costate vector is passed to the gradient module to evaluate the aerodynamic gradient. Then, the structural gradient is calculated and added to the aerodynamic gradient to form the overall gradient. The steepest descent method is used with a small step size to guarantee that the solution will converge to the optimum point. The design cycle is shown in figure 4.

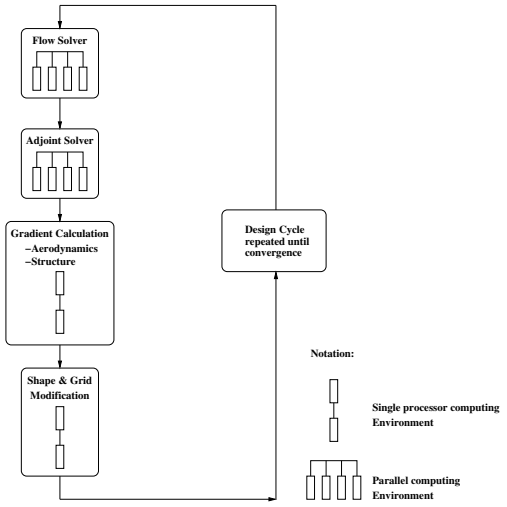

Figure 4. Design cycle

V. Flow solver and adjoint solver

The flow solver and the adjoint solver chosen in this work are codes developed by Jameson et al.[24,13,25,26] The flow solver solves the three dimensional Navier-Stokes equations by employing the JST scheme, together with a multistage explicit time stepping scheme. Rapid convergence to a steady state is achieved via variable local time steps, residual averaging, and a full approximation multi-grid scheme. The adjoint solver solves the corresponding adjoint equations using similar techniques to those of the flow solver. In fact much of the software is shared by the flow and adjoint solvers.

[a] Studies[23] have shown that, for the design purpose, only a 3 order of magnitude drop in the residual of the flow calculation and only a 2 order of magnitude drop in the residual of the adjoint calculation are sufficient.

VI. Results

A. Validation of aerodynamic and structural gradients with respect to planform variables

To verify the accuracy of the aerodynamic and structural gradients with respect to planform variables calculated by the adjoint method, we compare the adjoint gradients with those from the finite-difference methods. For the purpose of comparison, calculations are performed at a fixed angle of attack to eliminate the effect of pitch variation on the gradient. The case chosen is the Boeing 747 wing-fuselage combination at Mach 0.86, and wing angle of attack 2 degrees. The computational mesh is shown in figure 5.

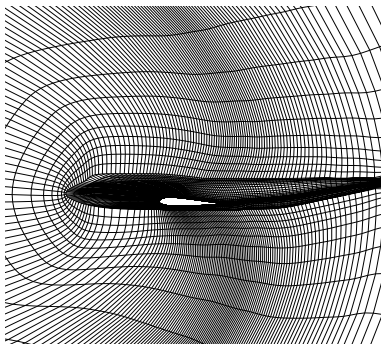

Figure 5. Computational Grid of the B747 Wing Fuselage. Mesh size 256x64x48.

The gradients with respect to the planform variables are calculated using both the adjoint and the finite-difference methods. A forward differencing technique is used for the finite-difference method with a moderate step size of 0.1% of planform variables to achieve accurate gradient with both small discretization and cancellation errors. The flow and adjoint solvers are run until both solutions converge five order of magnitude.

Figure 6 over-plots gradients from two methods for both drag and structural weight. The plots show that the gradients agree quite well.

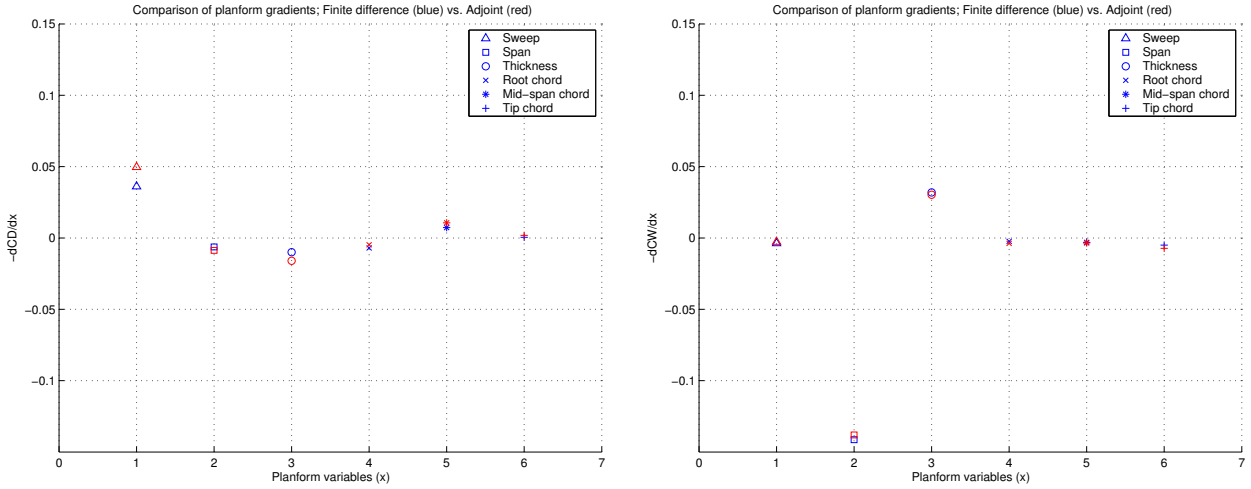

(a) Gradient of C_D

(b) Gradient of C_W

Figure 6. Comparison between adjoint and finite-difference gradient with respect to planform variables.

B. Redesign of Boeing 747 wing

We present results to show that the optimization with a trade-off between drag and structural weight results in a practical design. In these calculations the flow was modeled by the Reynolds Averaged Navier-Stokes equation, with a Baldwin Lomax turbulence model. This turbulence model was considered sufficient because the design point was at cruise condition with attached flow. The case chosen was the Boeing 747 wing fuselage combination at normal cruising Mach 0.85 and a lift coefficient $C_L = 0.45$.

As a reference point, we first modified only the wing sections to eliminate the shock drag, while planform of the baseline B747 was kept unchanged. Figure 7 shows the redesigned calculation. Here the drag was reduced from 137 counts to 127 counts (7.3% reduction) and the weight was slightly reduced from 498 counts to 494 counts (0.8%) in 30 design iterations with relatively small changes in the section shape.

Next, we allowed section changes together with variations of sweepback, span, root chord, mid-span chord, and tip chord. However, due to high computational cost of the Navier-Stroke optimization, the planform was initially designed by the inviscid method.[16] The sections of this wing were then optimized with a viscous

method while keeping planform constant, shown in figure 8. The inviscid-planform had a starting drag and weight of 129 and 472 counts respectively, which were already less than those of the baseline B747 (C_D 137 counts and C_W 498 counts), indicating that the inviscid-planform was a good starting point for the viscous optimization. To investigate contribution from shock drag, we performed section modification at fixed planform. In 30 design cycles, the drag was reduced to 120 counts, while the structural weight was constant.

Now, we implement both section and planform optimization in viscous design, using the starting wing of figure 8 as a starting point. Figure 9 shows the effect of allowing changes in sweepback, span, root chord, mid-span chord, and tip chord. The parameter α_3/α_1 was chosen according to formula (29) such that the cost function corresponded to maximizing the range of the aircraft. In 30 design iterations the drag was reduced to 117 counts (14.5% reduction from the baseline B747), while the dimensionless structure weight was decreased to 464 counts (6.1% reduction), which corresponded to a reduction of 5,500 lbs. The planform changes are shown in figure 10. This viscous redesigned wing has less drag and structural weight than that of the optimized fixed planform.

Both results from the inviscid and viscous planform optimization suggest a similar trend to yield large drag reduction, while maintaining low structural weight:

- Increase wing span to reduce vortex drag,
- Reduce sweep but increase section-thickness to reduce structural weight,
- Use section optimization to minimize shock drag.

Although the suggested trend tends to increase the wing area, which increases the skin friction drag, the pressure drag drops at a faster rate, dominating the trade-off. Overall, the combined results yields improvements in both drag and weight.

C. Pareto front

The problem of optimizing both drag and weight can be treated as a multi-objective function optimization as in this paper. A different choice of α_1 and α_3 will result in a different optimum shape. The optimum shapes should not dominate each other, and therefore lie on the Pareto front. The Pareto front can be very useful to the designer because it represents a set which is optimal in the sense that no improvement can be achieved in one objective component that does not lead to degradation in at least one of the remaining components.

Figure 11 shows the effect of the weighting parameters (α_1, α_3) on the optimal design. As before the design variables are sweepback, span, chords, section thickness, and mesh points on the wing surface. In figure 11 each point corresponds to an optimal shape for one specific choice of (α_1, α_3). By varying α_1 and α_3, we capture a Pareto front that bounds all the solutions. All points on this front are acceptable solutions, and choosing the final design along this front depends on the nature of the problem and several other factors. The optimum shape that corresponds to the maximum Breguet range is also marked in the figure.

VII. Conclusion

This paper develops and validates an aerodynamic design methodology based on the Navier-Stokes equations for planform optimization. A model for the structural weight is included in the design cost function. The results of optimizing a wing-fuselage of a commercial transonic transport aircraft has highlighted the importance of the structural weight model and the the viscous effects on the design process.

The trade-off between the structural cost function and the aerodynamic cost function prevents an unrealistic result and leads to a useful design. The inclusion of viscous effects increases the level of realism of the design. Methods of combining drag and wing weight also provide the designer a better opportunity to choose the final optimum shape.

Results indicate that the shape changes in the section needed to improve the transonic wing design are quite small. However, in order to obtain a true optimum design larger scale changes such as changes in the wing planform (sweepback, span, chord, and taper) should be considered. Because these directly affect the structure weight, a meaningful result can only be obtained by considering a cost function that takes account of both the aerodynamic characteristics and the weight.

When maximizing the range of the aircraft, both the inviscid and viscous optimization follow the same trend; increasing span to reduce the vortex drag, decreasing sweep and thickening wing-sections to reduce structural weight, and modifying airfoil sections to minimize the shock drag. In addition this trend suggests a way to reduce the computational cost by redesign in two steps; first optimize by the inviscid optimizer which is less expensive, then use the viscous optimizer to finalize the geometry.

VIII. Acknowldegment

This work has benefited greatly from the support of the Air Force Office of Science Research under grant No. AF F49620-98-1-2004.

References

[1]Martins, J. R. R. A., *A Coupled-Adjoint Method for High-Fidelity Aero-Strucural Optimization*, Ph.D. thesis, Stanford University, Stanford, CA, 2002.

[2]Bischof, C., Carle, A., Corliss, G., Griewank, A., and Hovland, P., "Generating derivative codes from Fortran programs," *Internal report MCS-P263-0991*, Computer Science Division, Argonne National Laboratory and Center of Research on Parallel Computation, Rice University, 1991.

[3]Lions, J., *Optimal Control of Systems Governed by Partial Differential Equations*, Springer-Verlag, New York, 1971, Translated by S.K. Mitter.

[4]Pironneau, O., *Optimal Shape Design for Elliptic Systems*, Springer-Verlag, New York, 1984.

[5]Jameson, A., "Aerodynamic Design via Control Theory," *Journal of Scientific Computing*, Vol. 3, 1988, pp. 233–260.

[6]Jameson, A., "Optimum Aerodynamic Design Using CFD and Control Theory," *AIAA paper 95-1729*, AIAA 12th Computational Fluid Dynamics Conference, San Diego, CA, June 1995.

[7]Jameson, A., "Re-engineering the Design Process Through Computation," *AIAA paper 97-0641*, 35th Aerospace Sciences Meeting and Exhibit, Reno, Nevada, January 1997.

[8]Reuther, J., Alonso, J. J., Vassberg, J. C., Jameson, A., and Martinelli, L., "An Efficient Multiblock Method for Aerodynamic Analysis and Design on Distributed Memory Systems," *AIAA paper 97-1893*, June 1997.

[9]Reuther, J., Alonso, J., Rimlinger, M., and Jameson, A., "Aerodynamic Shape Optimization of Supersonic Aircraft Configurations via an Adjoint Formulation on Parallel Computers," *AIAA paper 96-4045*, 6th AIAA/NASA/ISSMO Symposium on Multidisciplinary Analysis and Optimization, Bellevue, WA, September 1996.

[10]Baysal, O. and Eleshaky, M. E., "Aerodynamic Design Optimization Using Sensitivity Analysis and Computational Fluid Dynamics," *AIAA paper 91-0471*, 29th Aerospace Sciences Meeting, Reno, Nevada, January 1991.

[11]Anderson, W. K. and Venkatakrishnan, V., "Aerodynamic Design Optimization on Unstructured Grids with a Continuous Adjoint Formulation," *AIAA paper 97-0643*, 35th Aerospace Sciences Meeting and Exhibit, Reno, Nevada, January 1997.

[12]Jameson, A. and Martinelli, L., "Aerodynamic Shape Optimization Techniques Based on Control Theory," Tech. rep., CIME (International Mathematical Summer Center), Martina Franca, Italy, 1999.

[13]Jameson, A., "A perspective on computational algorithms for aerodynamic analysis and design," *Progress in Aerospace Sciences*, Vol. 37, 2001, pp. 197–243.

[14]Leoviriyakit, K. and Jameson, A., "Aerodynamic Shape Optimization of Wings including Planform Variables," *AIAA paper 2003-0210*, 41st Aerospace Sciences Meeting & Exhibit, Reno, Nevada, January 2003.

[15]Leoviriyakit, K., Kim, S., and Jameson, A., "Viscous Aerodynamic Shape Optimization of Wings including Planform Variables," *AIAA paper 2003-3498*, 21st Applied Aerodynamics Conference, Orlando, Florida, June 2003.

[16]Leoviriyakit, K. and Jameson, A., "Aero-Structural Wing Planform Optimization," *AIAA paper 2004-0029*, 42nd Aerospace Sciences Meeting & Exhibit, Reno, Nevada, January 2004.

[17]Leoviriyakit, K. and Jameson, A., "Case Studies in Aero-Structural Wing Planform and Section Optimization," *AIAA paper 2004-5372*, 22nd Applied Aerodynamics Conference and Exhibit, Providence, Rhode Island, August 2004.

[18]Jameson, A., "Automatic Design of Transonic Airfoils to Reduce the Shock Induced Pressure Drag," *Proceedings of the 31st Israel Annual Conference on Aviation and Aeronautics, Tel Aviv*, February 1990, pp. 5–17.

[19]Jameson, A., "Optimum Aerodynamic Design using Control Theory," *Computational Fluid Dynamics Review*, 1995, pp. 495–528.

[20]Jameson, A., "Aerodynamic Shape Optimization Using the Adjoint Method," 2002-2003 lecture series at the von karman institute, Von Karman Institute For Fluid Dynamics, Brussels, Belgium, Febuary 3-7 2003.

[21]Wakayama, S., "Lifting Surface Design Using Multidisplinary Optimization," Tech. rep., Stanford University Doctoral Dissertation, Stanford, CA, 1994.

[22]Kroo, I. M., "Design and Analysis of Optimally-Loaded Lifting Systems," *AIAA paper 1984-2507*, October 1984.

[23]Kim, S., Alonso, J. J., and Jameson, A., "A Gradient Accuracy Study for the Adjoint-Based Navier-Stokes Design Method," *AIAA paper 99-0299*, AIAA 37th Aerospace Sciences Meeting & Exhibit, Reno, NV, January 1999.

[24]Jameson, A., Martinelli, L., and Pierce, N. A., "Optimum Aerodynamic Design Using the Navier-Stokes Equations," *Theoretical and Computational Fluid Dynamics*, Vol. 10, 1998, pp. 213–237.

[25]Jameson, A., "Analysis and Design of Numerical Schemes for Gas Dynamics 1, Artificial Diffusion, Upwind Biasing, Limiters and their Effect on Multigrid Convergence," *Int. J. of Comp. Fluid Dyn.*, Vol. 4, 1995, pp. 171–218.

[26]Jameson, A., "Analysis and Design of Numerical Schemes for Gas Dynamics 2, Artificial Diffusion and Discrete Shock Structure," *Int. J. of Comp. Fluid Dyn.*, Vol. 5, 1995, pp. 1–38.

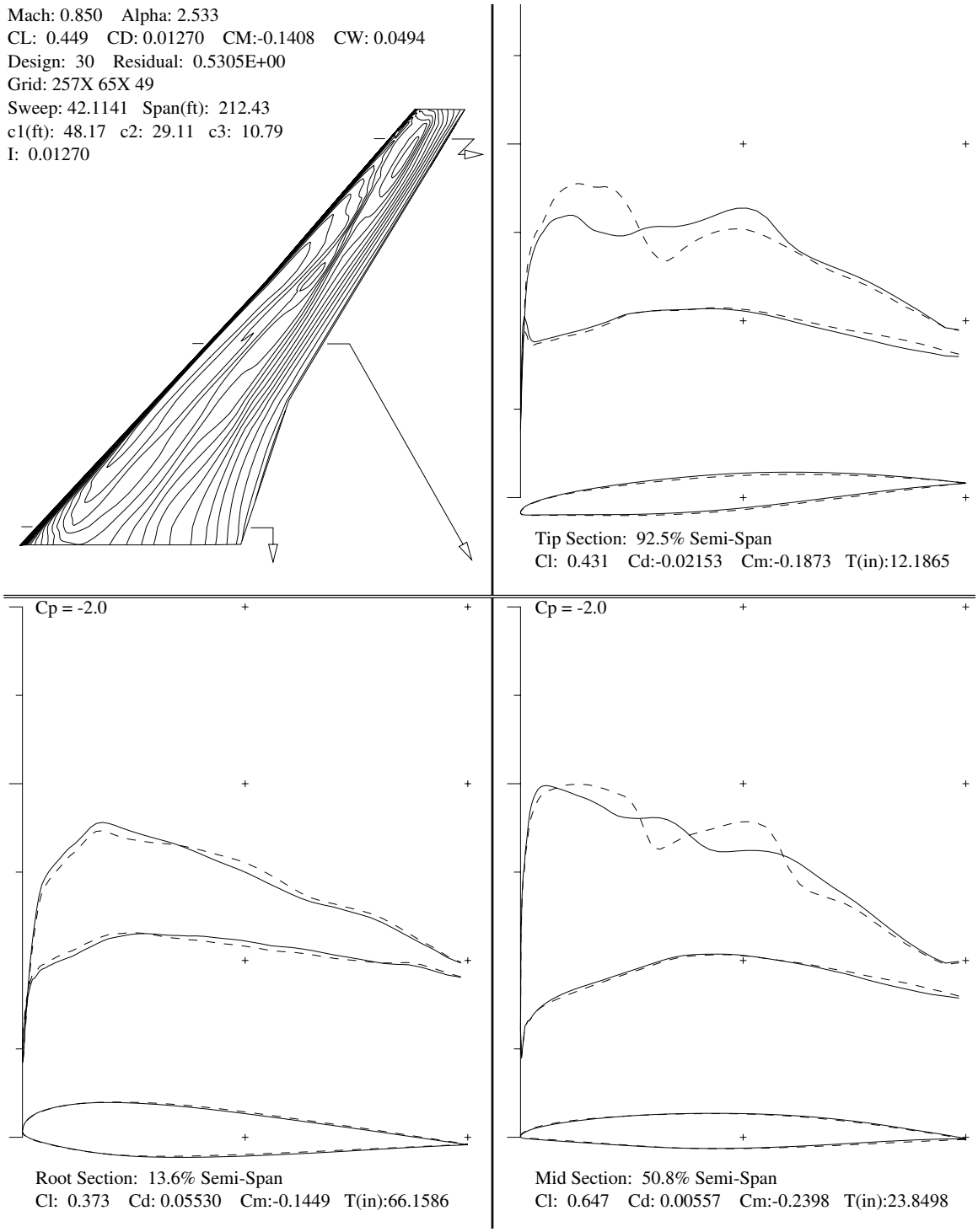

Figure 7. Wing-section optimization of Boeing 747 at fixed baseline-planform. Dash and solid lines represent pressure distributions of the baseline Boeing 747 and redesigned configuration respectively.

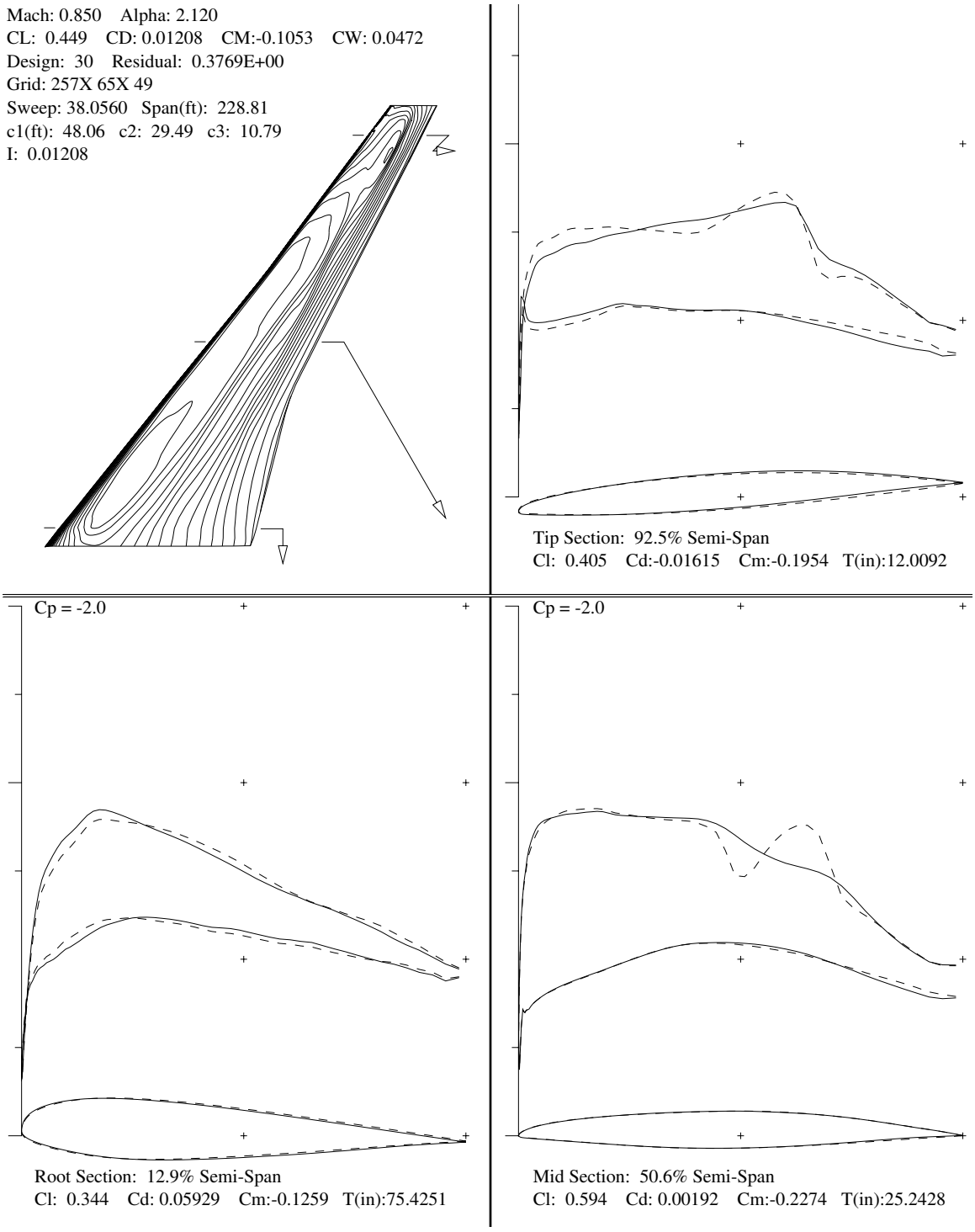

Figure 8. Wing-section optimization of Boeing 747 at fixed inviscid-optimized planform. The optimized planform from reference[16] is used as a starting point and no modification is made to the planform. The wing-sections are redesigned to alleviate the shock drag. Dash and solid lines represent pressure distributions of the starting and redesigned configurations respectively.

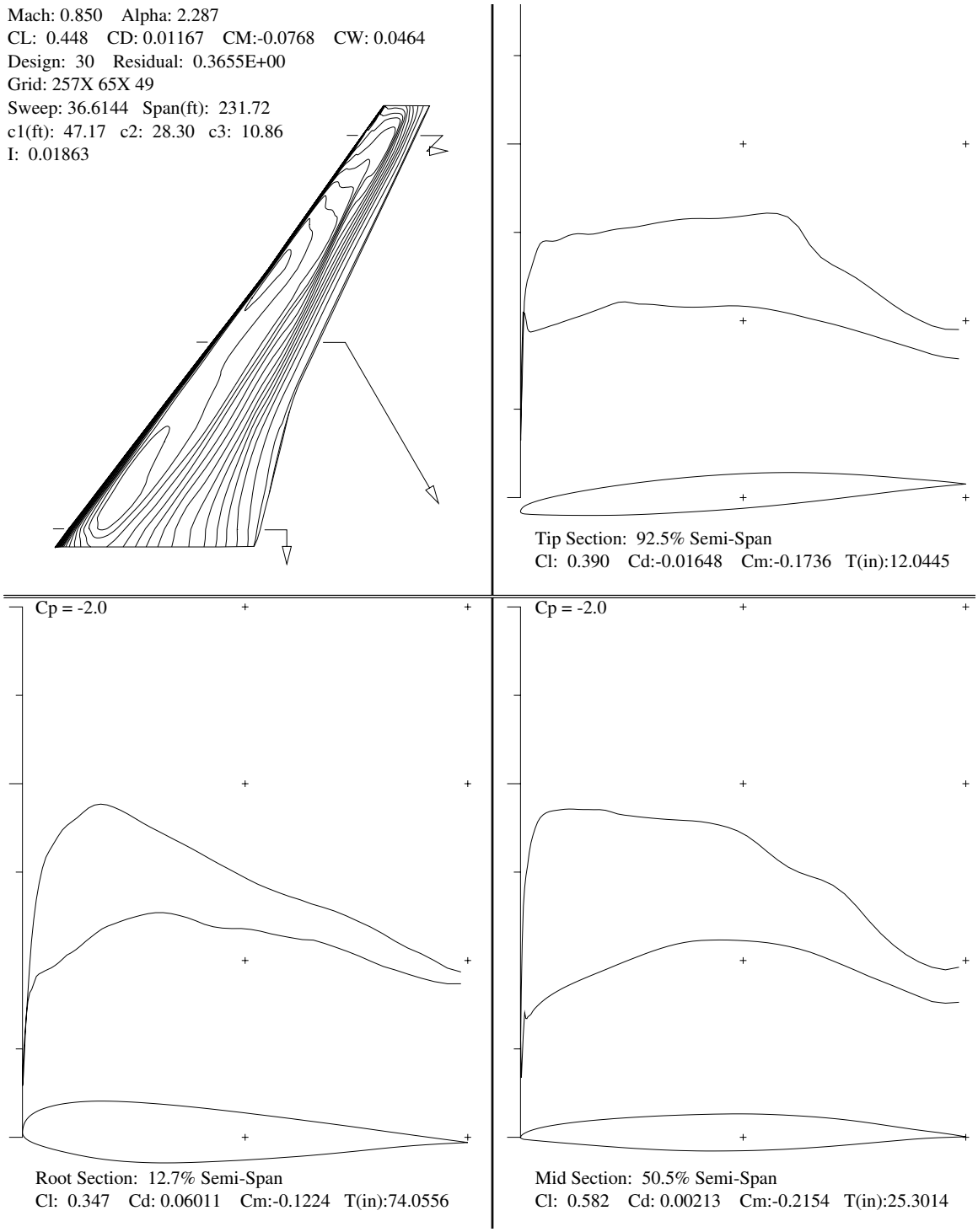

Figure 9. Complete optimization of Boeing 747. Both wing-section and planform are optimized to maximize the Braguet range, using inviscid-optimized planform as a starting points.

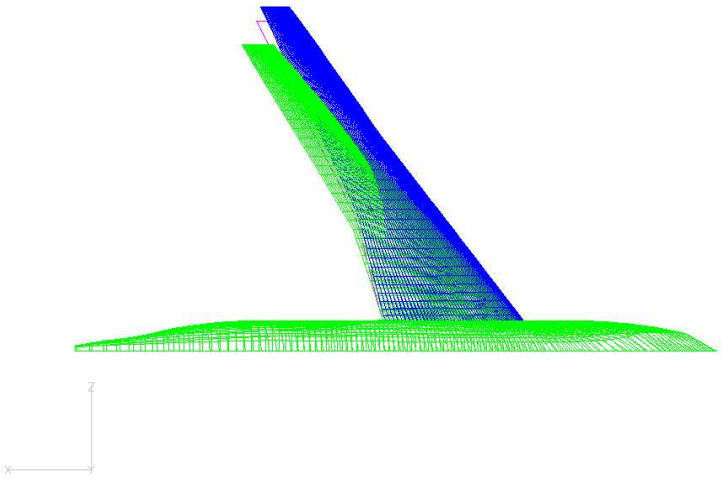

Figure 10. Superposition of the baseline B747 (green/light) and the optimized secton-and-planform geometry (blue/dark). The optimized-planform from inviscid calculation is also superimposed (magenta).

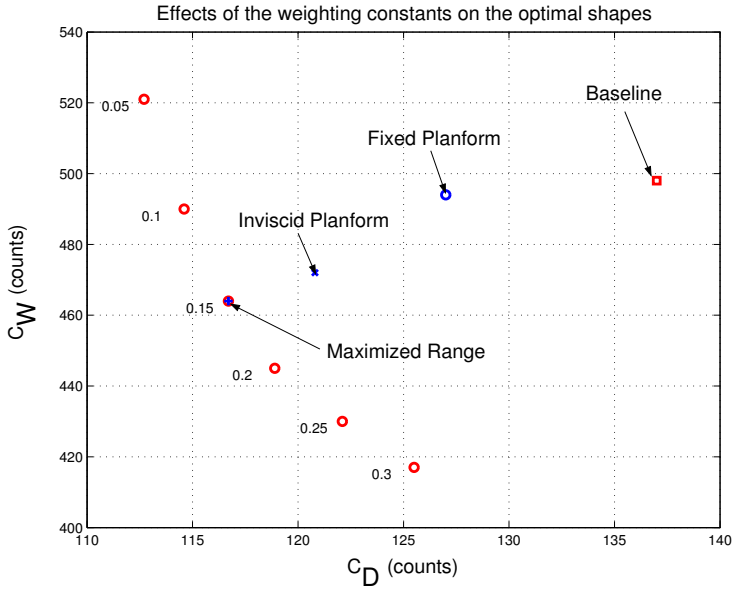

Figure 11. Pareto front of section and planform modifications. The ratios of $\frac{\alpha_3}{\alpha_1}$ are marked for each optimal point.